Appl. Phys. B 84, 269–273 (2006)
DOI: 10.1007/s00340-006-2206-1

Applied Physics B
Lasers and Optics

M.A. NOGINOV✉
G. ZHU
C. SMALL
J. NOVAK

Neodymium random laser with external mirrors

Center for Materials Research, Norfolk State University, 700 Park Ave., Norfolk, VA 23504, USA

Received: 23 December 2005
Published online: 19 April 2006 •

ABSTRACT We have studied the influence of the front and the rear mirrors on the emission properties of neodymium random lasers at different thicknesses of the powder layer. Introduction of external mirrors drastically reduces the lasing threshold of the random laser, with the effect of the front mirror being more dominant. External mirrors also influence the location of the stimulated emission region within the powder volume. The experimental results are in a good agreement with the results of the Monte-Carlo simulation.

PACS 42.55.Zz; 66.30.Pa

1 Introduction

Random lasers are miniature sources of stimulated emission in which the feedback is provided by scattering in a gain medium. First proposed by Letokhov in the late 60's [1] and experimentally demonstrated in 80's [2], random lasers have currently evolved into a large research field. The recent review of random lasers can be found in [3].

Since scattering provides the feedback in random lasers, they do not require any external cavity or mirrors. However, can external mirrors enhance the performance of random lasers? The answer is yes, if mirrors are positioned close enough to the gain medium and help to increase the feedback of stimulated emission or the efficiency of utilization of pumping. The random laser with one mirror, which had high transmission at the pumping wavelength and high reflection at the stimulated emission wavelength, was demonstrated in [4]. It has been shown that the mirror helps to reduce the threshold by $\sim 25\%$ and increase the slope efficiency by $\sim 30\%$. The relatively moderate improvement was explained by the fact that the mirror and the laser powder in [4] were separated by a 1 mm thick wall of the cuvette.

In [5], a one-mirror random laser has been studied theoretically. It has been shown that the mirror helps to reduce the laser threshold dramatically, especially in the systems operating in the localized regime, where the lasing threshold is otherwise very difficult to reach by optical pumping. The calculations predicted more than tenfold reduction of the threshold in a low-loss system [5]. The proposed threshold decrease was due to a better overlap between the pumped region and the lasing modes, as well as the different eigenmode structure of the half-closed system. In [6], a similar one-mirror setup was used to demonstrate first quasi-cw random laser based on compressed Nd:YAG powder. As it was shown in [7], an external mirror can enhance the output of a random laser (based on 300–350 nm films of ZnO nanoparticles excited with the third harmonic of picosecond Nd:YAG laser) not only when it is positioned in the front of the sample, but also in its rear.

✉ Fax: 757-823-9054, E-mail: mnoginov@nsu.edu

2 Experimental studies

In this work, we have studied the dependence of the random laser threshold in $NdSc_3(BO_3)_4$ powder on the presence of external mirrors and the thickness of the powder layer in three different configurations:

Setup #1 – the layet of powder was restricted by glass slabs from the front and from the back.

Setup #2 – the random laser had a glass wall in the front and a gold mirror in the rear (gold mirror reflected $\sim 58\%$ of light intensity at $\lambda = 0.53\,\mu$m and $\sim 98\%$ at $\lambda = 1.06\,\mu$m).

Setup #3 – the random laser had a dielectric mirror in the front, which transmitted pumping light and reflected stimulated emission light, and a gold mirror in the rear. (At $\lambda = 1.06\,\mu$m, the dielectric mirror had 100% reflectivity at 45° incidence, its reflection coefficient averaged over the solid angle 2π was estimated to be equal to 80%. At $\lambda = 0.53\,\mu$m, the reflection coefficient of the dielectric mirror, at normal incidence, was equal to 10%).

The powders were loaded in the custom-designed wedge-shaped containers, which allowed continuous tuning of the thickness of the powder between 0 and 4 millimeters, by sliding the container in the direction perpendicular to the pumping beam. The powder was pumped with Q-switched pulses of a frequency-doubled Nd:YAG laser ($t_{\text{pulse}} = 10$ ns, $\lambda_{\text{pump}} = 532$ nm). The diameter of the pumped spot d, which was determined using a knife-edge technique, was varied between 0.4 and 1.1 millimeters. In different particular experiments, it could be smaller or larger than the thickness of the powder layer. (In the measurement of d, the strip of masking aluminum foil (knife edge) was attached to the inner surface of the front glass slab, Fig. 1.)

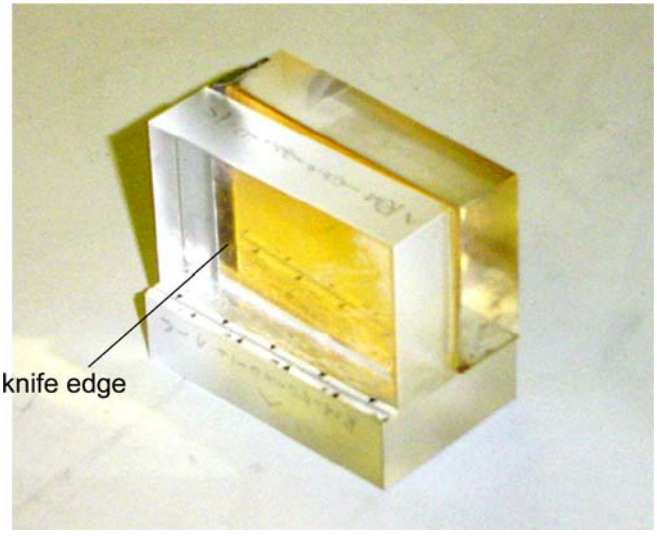

FIGURE 1 Wedge-shaped experimental cuvette

When the pumping energy exceeded some critical threshold level, the duration of the emission pulse(s) shortened from microseconds to nanoseconds, the emission spectrum narrowed to a single line, and the peak emission intensity increased dramatically. This behavior is typical of neodymium random lasers [2]. Experimentally, we recorded random laser pulses and plotted time-integrated emission signals versus pumping energy to obtain input–output curves, Fig. 2. The laser thresholds were determined from the input–output curves and plotted versus thickness of the powder layer for the three setups studied.

As it was shown in [8, 9], the threshold in neodymium random lasers is approximately proportional to the diameter of the pumped spot d. Although this was not exactly the case of setup #3, we divided the experimentally measured thresholds by the values of d and averaged the results obtained at different diameters of the pumped spot in order to reduce the scatter of the experimental data. The data treated this way are summarized for all three setups in Fig. 3a. As it follows from Fig. 3a,

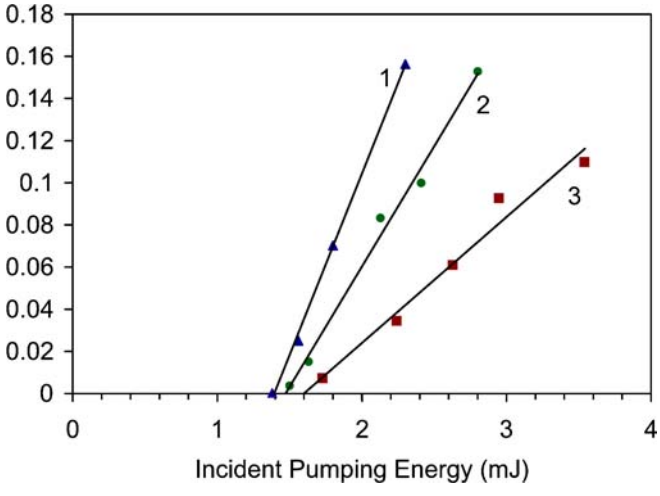

FIGURE 2 Representative input–output curves obtained in setup # 3. The thickness of the powder layer: 1.57 mm (1), 0.63 mm (2), and 0.29 mm (3), $d = 0.8$ mm

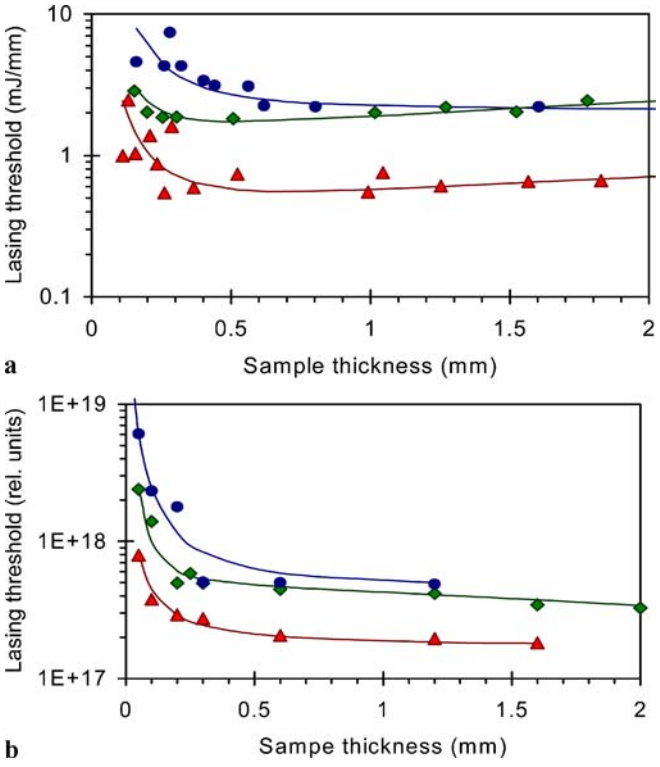

FIGURE 3 Dependence of the lasing threshold on the thickness of the pumped layer in setups #1 (*circles*), #2 (*diamonds*), and #3 (*triangles*). In (**a**), experimental threshold energy is normalized to the diameter of the pumped spot. When the thickness of the powder layer was smaller than 0.1 mm, the lasing threshold could not be reached even at significant increase of the pumping energy. The calculated results are shown in (**b**). *Solid lines* are guides for eye

(i) the thresholds are significantly increased when the thickness of the powder layer is getting smaller than 0.25 mm, (ii) the threshold is decreased with the addition of the gold mirror to the rear (this effect is clearly seen at relatively small thickness of the powder layer) and is significantly reduced further with the addition of the dielectric mirror to the front, and (iii) in setups #2 and #3, the threshold is slightly increased with the increase of the distance between the pumped volume and the gold mirror.

3 Monte-Carlo simulations

The behavior of a random laser in three different configurations above was investigated numerically by using 1D model of lasing cells separated by partially reflecting walls, Fig. 4a. As it has been shown in [10], this model adequately describes the behavior of neodymium random lasers with incoherent feedback. The length of each cell was assumed to be equal to 1 μm (characteristic particle size) and the average reflection coefficient of the cell wall ($R = 0.13$) corresponded to $l_t = 7$ μm, the value of the transport mean free path common to neodymium random lasers [11] and close to that in our experiment. In the Monte-Carlo simulation, we first sent to the strip (from the front end) a flux of pumping photons. Driven by a random function generator, each photon could be reflected by the wall between the cells, transmitted to the next cell, or absorbed inside the cell. The absorption probability in the model corresponded to the known absorption coefficient at

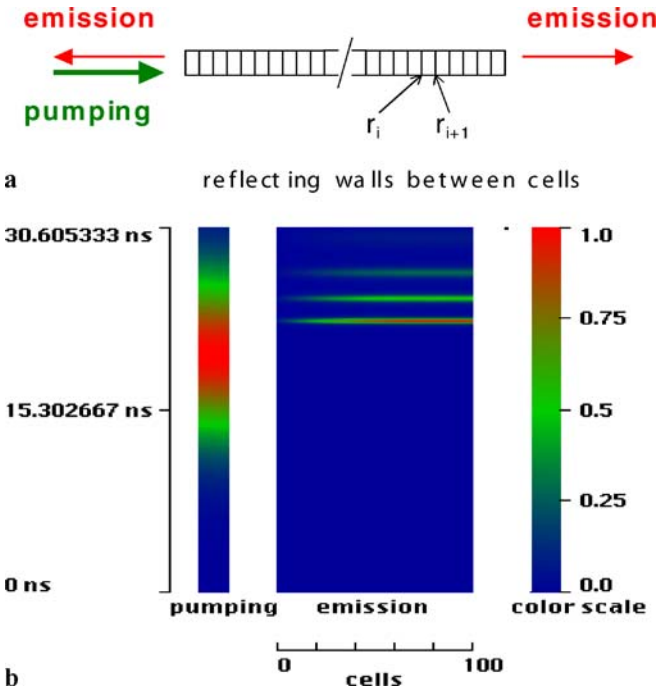

FIGURE 4 (**a**) 1D strip of lasing volumes modeled in Monte-Carlo calculations. (**b**) Position-dependent kinetics of stimulated emission calculated for setup #2. The color scale is shown on the right. The time profile of the pumping pulse is shown on the left

$\lambda = 532$ nm in the $NdSc_3(BO_3)_4$ powder with the filling factor 55%, 10.9 cm^{-1} [12]. This procedure gave us an exponential distribution of absorbed pumping energy in the system.

We then calculated the dynamics of stimulated emission in such system excited with 10 ns Gaussian-shaped pumping pulses. According to [12, 13], stimulated emission of neodymium random lasers can be adequately described by the system of rate equations for the population inversion n and the energy density of radiated photons E:

$$\frac{dn}{dt} = \frac{P(t)}{h\nu_p S l_p} - \frac{n}{\tau} - \frac{E}{h\nu_e} c\sigma_e n \tag{1a}$$

$$\frac{dE}{dt} = -\frac{E}{\tau_{res}} + \frac{\zeta n}{\tau} h\nu_e + Ec\sigma_e n\,, \tag{1b}$$

where $P(t)/S$ is the pumping power density; l_p is the depth of the pumped layer (Sl_p is the pumped volume); σ_e is the emission cross section, $h\nu_p$ ($h\nu_e$) is the photon energy at the pumping (emission) wavelength; τ is the spontaneous decay time determined by the spontaneous emission, multiphonon relaxation, and cross-relaxation; $\zeta n/\tau$ is the rate with which spontaneously emitted photons populate lasing mode(s); τ_{res} is the photon residence time in scattering medium; and c is the speed of light.

The photon residence time in the system was determined by the transmission of the walls, the size of the strip, and the position inside the strip where the emission photon was "born". The front and the rear mirrors were modeled by assigning appropriate reflection coefficients to the outer walls of the first and the last cells of the strip. The spectroscopic parameters used in the model corresponded to $NdSc_3(BO_3)_4$ powder [12]. Since neodymium random lasers have very low degree of coherence, we, in accord with [10], did not include in the model any coherence or wave phenomena. The typical calculated dynamics of stimulated emission in the strip of lasing cells is shown in Fig. 4b. The calculated spiked behavior of emission above the threshold was similar to that observed experimentally (see also [12]).

To calculate the number of output photons, which exited the strip through the front (rear) end, we determined the outbound photon flux in the first (last) cell and multiplied it by the transmission coefficient of the corresponding outer wall. By calculating the values of the stimulated emission output at different pumping energies, we were able to plot input–output curves and determine lasing thresholds for each setup and several different lengths of the strip studied. The results of the calculations are summarized in Fig. 3b. The calculated results have a fairly good agreement with the experimental ones. In fact:

(i) All three calculated curves show significant increase of the threshold at small thickness of powder layer. This result can be explained as follows. When the layer of powder is getting thin, it first fails to provide adequate feedback for the stimulated emission and, at further reduction of the thickness, it becomes transparent for pumping.

(ii) The threshold is reduced when the gold mirror is installed in the rear and is lowered even further when the dielectric mirror is installed in the front. This result can also be easily understood, since both the rear and the front mirrors increase the photon residence time in the pumped volume.

The overall effect of the front mirror appears to be larger than that of the rear mirror. Moreover, as follows from Fig. 3a (diamonds and triangles), the effect of the rear mirror vanishes at large thickness of the powder layer, > 0.5 mm, causing an increase of the threshold energy in setups #2 and #3 with the increase of the sample thickness. The latter effect is not predicted by 1D diffusion model. We believe that the disagreement between the experiment and the 1D calculation above is caused by three-dimensional nature of photon propagation in thick layers of powder: the flux of emission photons propagating from the pumped volume to the rear mirror and then back to the pumped volume constantly increases in diameter. This makes the feedback inefficient at long propagation distances. In this case, a random laser does not notice the presence of the rear mirror.

As expected, the system switches from 1D behavior to 3D behavior at the thickness of the powder layer (~ 0.5 mm), which is approximately equal to the diameter of the pumped spot. The reduction of the threshold caused by the presence of the dielectric mirror in the front of the sample is larger than that due to the rear mirror; however, it is smaller (in experiment and calculation) than that predicted in [5]. The relatively moderate reduction of the threshold is explained by high ($\sim 20\%$) transmission of the dielectric mirror integrated over the solid angle 2π. In fact, many commercially available dielectric mirrors have high reflectivity at some specified angle of incidence and much lower reflection coefficients at other angles.

The calculated dependence of the random laser threshold on the reflectivity of the front mirror is depicted in Fig. 5. (In this calculation, the thickness of the powder layer corre-

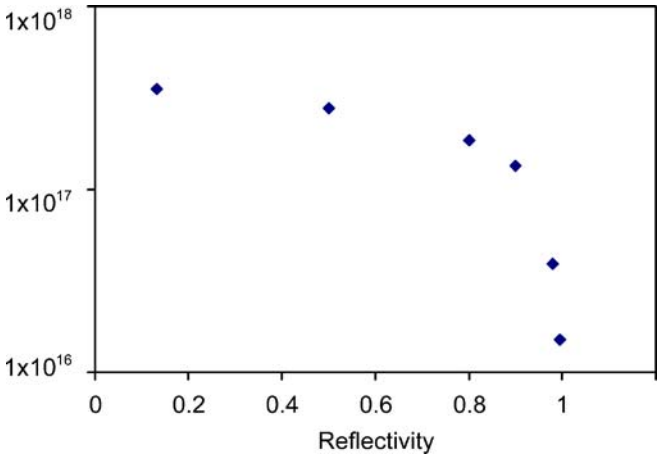

FIGURE 5 Lasing threshold as a function of the front mirror reflectivity in a strip consisting of 1200 lasing cells

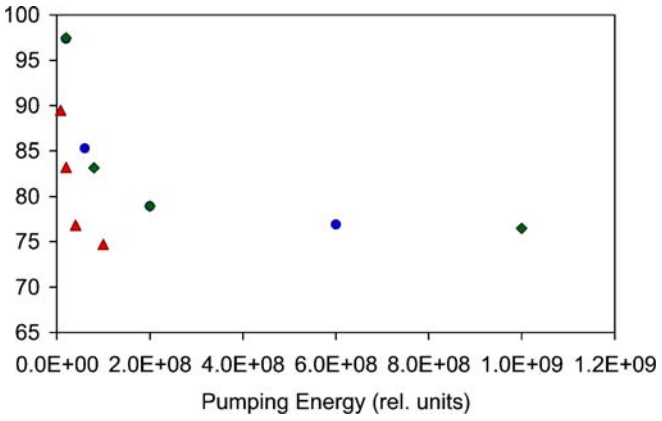

FIGURE 7 Center of gravity of the rate of generation of stimulated emission X_0 as a function of the pumping energy (setup #1 – circles, setup #2 – diamonds, and setup #3 – triangles, 1200 cells)

sponded to 1200 cells and no mirror was present in the rear of the sample.) As it follows from Fig. 5, the random laser threshold can be reduced more than twenty-fold when the angle-averaged reflectivity of the mirror is equal to 99.5%.

An ideal random laser mirror should have high (100%) reflection at all angles except for a very small solid angle surrounding the direction of normal incidence. This would not only significantly reduce the random laser threshold but also improve its brightness and directionality.

If both front and rear walls of the strip (front and rear mirrors surrounding the layer of powder) can partially transmit random laser emission, the ratio of the light intensity radiated to the front and to the rear will depend on the position of the stimulated emission region within the sample. The ratio of light intensities emitted to the front and to the rear of the sample calculated for the three setups studied is shown in Fig. 6. (In the case of setups #2 and #3, we assumed that the back mirror was not the gold mirror reflecting 98% and absorbing 2% of emission but a lossless dielectric mirror transmitting 2% of incident light.) One can see that with the increase of the pumping energy, the "front-to-rear" ratio increases, which implies that the effective stimulated emission region shifts toward the front wall. This result is in agreement with that of [14], where we have predicted that in the front-pumped random laser operating in the diffusion regime, the stimulated emission is first achieved in the depth of the powder and only at higher pumping energies – in the layers adjacent to the surface.

If the distribution of the stimulated emission energy density $I(x)$ and the distribution of the population inversion $n(x)$ within the sample are known, then the shape and the position of the effective source of stimulated emission

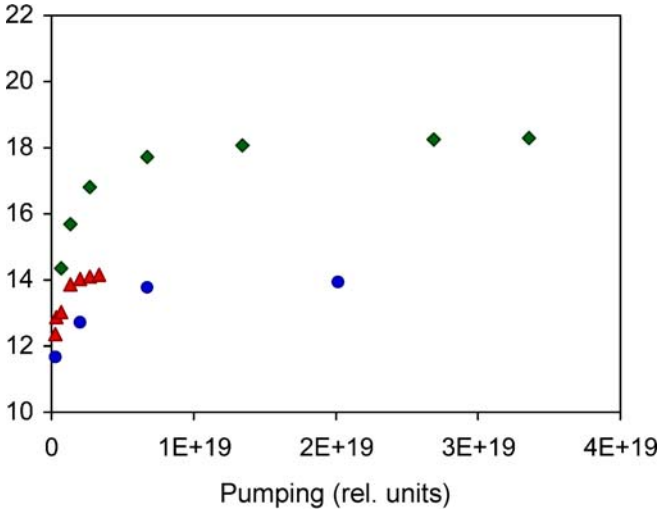

FIGURE 6 Dependence of the front-to-rear emission ratio as the function of the pumping energy, calculated for the three setups studied (setup #1 – circles, setup #2 – diamonds, and setup #3 – triangles). The length of the strip is equal to 1200 cells

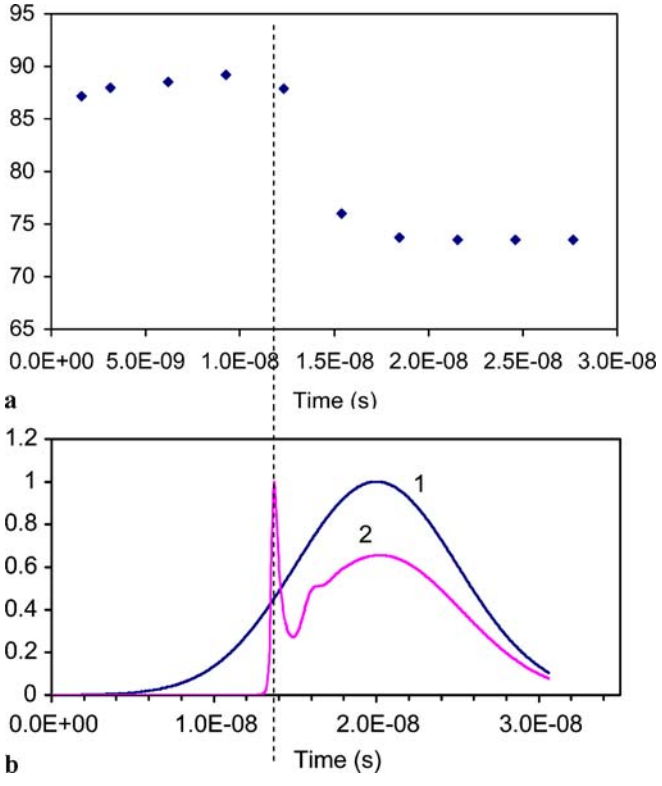

FIGURE 8 (**a**) Center of gravity of the rate of generation of stimulated emission X_0 as a function of time. (**b**) Pumping pulse (1) and stimulated emission kinetics (2) corresponding to the dynamics of X_0 in (**a**). (setup #3, 1200 cells)

(or the rate of generation of stimulated emission) can be described by the function $I(x)n(x)$ (here x is the position within the strip). Correspondingly, the 'center of gravity' X_0 of the stimulated emission source can be calculated as $X_0 = \int I(x)n(x)x\mathrm{d}x / \int I(x)n(x)\mathrm{d}x$.

According to Fig. 7 depicting the dependence of X_0 on the pumping energy, the effective time-averaged position of the stimulated emission source sharply relocates toward the front wall of the sample when the threshold is reached, in agreement with the data presented in Fig. 6. Figure 8a shows the relocation of the center of gravity of the stimulated emission source X_0 within one pumping pulse. According to Figs. 8a and 8b, the center of gravity X_0 moves sharply toward the front of the sample at the moment of time corresponding to the appearance of the first relaxation oscillation spike in the stimulated emission kinetics.

4 Summary

We have studied the effects of the front and the rare mirrors as well as the thickness of the powder sample on stimulated emission of neodymium random lasers. We have found that with or without mirrors, the threshold of stimulated emission dramatically increases when the thickness of the powder layer is getting smaller than several times the penetration depth of pumping (~ 40 μm [15]) or several tens times the transport mean free path (~ 7 μm [11]). The rear mirror can cause approximately two-fold reduction of the threshold when the thickness of the powder layer does not exceed the diameter of the pumped spot. Such mirrors can be inexpensive and easy to use in many random laser applications. The front dielectric mirror can cause a much stronger reduction of the threshold (up to 20 times). However, the reflection of such dielectric mirror integrated over the solid angle 2π should be large (very close to 100%).

ACKNOWLEDGEMENTS This work was supported by the NASA grants NCC-1-01049 and NCC-3-1035 and the NSF grant HRD-0317722.

REFERENCES

1 V.S. Letokhov, Sov. Phys. JETP **26**, 835 (1968)
2 V.M. Markushev, V.F. Zolin, C.M. Briskina, Sov. J. Quantum Electron. **16**, 281 (1986)
3 M.A. Noginov, *Solid-State Random Lasers* (Springer, printed in the USA, 2005) p. 235
4 M.A. Noginov, N. Noginova, S.U. Egarievwe, J.C. Wang, H.J. Caulfield, ICONO'98: Nonlinear Optical Phenomena and Coherent Optics in information Technologies, S.S. Chesnokov, V.P. Kandidov, N.I. Koroteev (Eds.), Proc. of SPIE Vol. **3733**, 223 (1999)
5 Y. Feng, K. Ueda, Phys. Rev. A. **68**, 025 803 (2003)
6 Y. Feng, J.-F. Bisson, J. Lu, S. Huang, K. Takaichi, A. Shirakawa, M. Musha, K. Ueda, Appl. Phys. Lett. **84**, 1040 (2004)
7 H. Cao, Y.G. Zhao, X. Liu, E.W. Seelig, R. Chang, P.H. Chang, Appl. Phys. Lett. **75**, 1213 (1999)
8 M. Bahoura, K.J. Morris, M.A. Noginov, Opt. Commun. **201**, 405 (2002)
9 M. Bahoura, K.J. Morris, G. Zhu, M. Noginov, IEEE J. Quantum Electron. **41**, 677 (2005)
10 M.A. Noginov, J. Novak, S. Williams, Phys. Rev. A **70**, 063 810 (2004)
11 M. Bahoura, M.A. Noginov, J. Opt. Soc. Am. B **20**, 2389 (2003)
12 M.A. Noginov, N.E. Noginova, H.J. Caulfield, P. Venkateswarlu, T. Thompson, M. Mahdi, V. Ostroumov, J. Opt. Soc. Am. B **13**, 2024 (1996)
13 M.A. Noginov, I.N. Fowlkes, G. Zhu, J. Novak, Phys. Rev. A. **70**, 043 811 (2004)
14 M.A. Noginov, J. Novak, D. Grigsby, G. Zhu, M. Bahoura, Opt. Express **13**, 8829 (2005)
15 M.A. Noginov, N. Noginova, S. Egarievwe, J.C. Wang, M.R. Kokta, J. Paitz, Opt. Mater. **11**, 1 (1998)